Applied Catalysis B: Environmental 166–167 (2015) 465–474

Contents lists available at ScienceDirect

Applied Catalysis B: Environmental

journal homepage: www.elsevier.com/locate/apcatb

Selective catalytic reduction of NO_x with C_3H_8 using Co-ZSM5 and Co-MOR as catalysts: A model to account for the irreversible deactivation promoted by H_2O

A. Martínez-Hernández [a,*], G.A. Fuentes [b], Sergio A. Gómez [b]

[a] Universidad Autónoma de Nuevo León, UANL, Facultad de Ciencias Químicas, Av. Universidad S/N, San Nicolás de los Garza, Ciudad Universitaria, C.P. 66451 N.L, Mexico
[b] Universidad Autónoma Metropolitana-Iztapalapa, Área de Ingeniería Química, A.P. 55-534, 09340 México, D.F., Mexico

ARTICLE INFO

Article history:
Received 6 August 2014
Received in revised form
14 November 2014
Accepted 29 November 2014
Available online 3 December 2014

Keywords:
NO_x reduction
Deactivation mechanism
Cation migration
Zeolites
Kinetics of deactivation

ABSTRACT

A deactivation mechanism and a model are proposed for the H_2O-induced deactivation of Co-ZSM5 and Co-MOR catalysts at high GHSV (150,000 and 90,000 h^{-1}) during Selective Catalytic Reduction of NO_x (SCR-NO_x). The model is based on the analysis of the deactivation curves, as well as DR UV-Vis and H_2-TPR, for the structural characterisation of the catalysts before and after long-term hydrothermal operation. We propose that Co^{2+} active sites are lost during deactivation by migration into the zeolite channels to isolated sites with low SCR-NO_x activity and by the formation of cobalt oxide crystallites (CoOx). This process is promoted by the presence of H_2O in the reaction medium. The deactivation curves can be modelled as resulting from a solid-state migration properly fitted using an equation for a packed bed reactor (PBR) coupled with the transformation of the cobalt sites in a reaction series $S_1 \rightarrow S_2 \rightarrow S_3$, with S_2 being the active sites for the SCR-NO_x reduction reaction. The numerical solution of this model was found to be in good match with our experimental data, suggesting that the re-arrangements of Co in both zeolites by H_2O promotion occurred under the same mechanism.

1. Introduction

For several years, the search for an adequate catalyst for NO_x reduction under lean-burn conditions has prompted the study of many materials. Zeolites, in particular, exchanged with cations of different transition metals, such as Cu, Co or Fe, have received much attention for their ability to efficiently reduce NO_x compounds using light hydrocarbons as a reducing agent [1–7]. Actually, the most promising catalysts for NH_3-SCR are iron and copper exchanged in zeolites that show high stability against deactivation in hydrothermal operation, as examples are iron exchanged in BEA zeolite [8] and copper exchanged in SSZ-13 zeolite [9]. However, the stability of this type of catalyst under the presence of water, which is unavoidable during practical application, is still an issue to be solved. The process whereby H_2O promotes deactivation is still unknown, since there is a strong dependence on the operating conditions, type and degree of cation exchange and zeolite type. For example, in a NH_3-SCR study using Fe-ZSM5, Brandenberger et al. [10] suggested that the thermal deactivation occurred by three parallel processes; (i) rapid dealumination of Al-OH-Si sites, (ii) rapid depletion of dimeric iron species and (iii) slow migration of isolated iron ions followed by dealumination. For Fe-BEA used as model catalyst for the same reaction, Shwan et al. [11] proposed that the deactivation proceeds in two steps; (i) milder ageing results in formation of oligomeric iron clusters in the zeolite pores, and hence decreasing the number of isolated ions, and (ii) severe ageing results in continuous migration and formation of larger iron particles. For Cu/SSZ-13 Gao et al. [12] found that Cu^{2+} migrates in H_2O presence, and forms moieties that block pore openings of the zeolite decreasing the efficiency of the catalysts. Vennestrom et al. [13] compared the deactivation of Cu-ZSM5 and Cu-IM-5 catalysts during NH_3-SCR, and proposed that during hydrothermal deactivation of both zeolites there are (i) a partial dealumination of Al associated with Cu species, (ii) then migration of copper and formation of CuO, resulting in a detached Al from the zeolite framework and formation of a Cu–Al phase that resembles $CuAl_2O_4$ species.

The studies mentioned above were carried out under accelerating deactivation conditions by heating the catalysts above of 600 °C in order to detect cation migration into the zeolite framework; however, this experimental condition also forced the dealumination of the zeolite catalysts. In the literature, there is a general

* Corresponding author. Tel.: +52 81 8329 4000, Ext.3443.
E-mail address: angel.martinezhn@uanl.edu.mx (A. Martínez-Hernández).

http://dx.doi.org/10.1016/j.apcatb.2014.11.059
0926-3373/

consensus that the deactivation of M-zeolite (M = Cu, Fe, or Co) catalysts at temperatures below 500 °C occurs mainly through modifications of the cation sites and not because of damage to the zeolite matrix (dealumination); relocation to low-activity sites and/or the formation of metal oxide moieties [14–16].

Among the transition metals studied to date, cobalt has also received attention due to its superior water resistance to copper when it is exchanged in ZSM5 [3,4,17]. Cobalt has also been probed in other types of zeolites, such as FER, BEA and MOR, showing high activity for the deNO_x reaction [17–22].

In the case of deNO_x reaction results, they are difficult to rationalise because the reported transient activity curves follow different trajectories. For example, Co-MOR deactivation usually follows an exponential decay with time on stream (TOS), whereas Co-ZSM5 catalysts follow a sigmoidal decay [15–23]. Also, in the available literature, there are a broad range of operating conditions used, making it quite difficult to correlate information and to determine the mechanism controlling deactivation. This indicates that there is still a need for more fundamental information on the deactivation of M-Zeolite deNO_x catalysts.

We chose then to study the deactivation of two cobalt-exchanged zeolite based catalysts (ZSM5 and MOR) during long-term lean NO_x reduction under the presence of water. A deactivation model based on the analysis of the deactivation curves, as well as on DR UV-Vis and H_2-TPR results is proposed. The numerical solution of this model was found to be in excellent agreement with the experimental data, suggesting that the re-arrangements of Co in both zeolites by H_2O promotion occurred under the same mechanism.

2. Experimental

2.1. Catalysts preparation

Co-ZSM5 catalysts were prepared by ion exchange of the Na-ZSM5 zeolite (Pentasil Zeocat: Si/Al = 37) with a solution of cobalt acetate (J.T. Baker) (0.01–0.02 M). The ion exchange slurry was kept at 80 °C for 24 h. After that, the slurry was filtered, and the solids obtained were washed with twice the amount of water used during the ion-exchange stage. For Co-MOR catalysts, the parent zeolite was Na-MOR (Zeolyst, SiO_2/Al_2O_3 = 13), and the same ion exchange procedure was carried out. The resultant amount of cobalt in the catalysts was measured by atomic absorption spectroscopy (Varian SpectrAA-20). Results are presented in Table 1.

2.2. Long-term catalytic tests

Long-term catalytic tests were performed in a quartz microreactor with online NO/NO_x analysis (Rosemount 951A or Eco Physics CLD 70S) and online GC (HP 5890 series II). Prior to the reaction tests, the catalysts were calcined at 500 °C in a muffle in the presence of static air. The feed stream consisted of 1250 ppm NO, 3250 ppm C_3H_8 and 4% (v/v) of O_2 in N_2 balance. The H_2O used ranged from 0 to 10% (v/v) and was introduced to the system by means of a syringe pump; all the lines were heated to evaporate the water before it reached the reactor. The total flow used was 150 cm^3/min, and the spatial velocity was set at 150,000 h^{-1} in the case of Co-ZSM5 (Reaction Temperature = T_r = 500 °C) and at 90,000 h^{-1} for Co-MOR (T_r = 450 °C). The difference in the space velocity arises from the fact that Co-MOR presented an immediate decrease in NO_x conversion from the beginning of the test, being more pronounced at elevated GHSV, preventing us from adequately track the deactivation curve with the TOS. The temperature used in each case corresponded to the maximum NO_x conversion observed for each catalyst in our programmed temperature reaction experiments.

Table 1
Chemical analysis of cobalt catalysts.

Sample	Co loading (wt%)	Co^{2+}/Al (atom/atom)	Na^+/Al (atom/atom)
Parent Na-ZSM5	–	–	0.81
Co-ZSM5-0.34	0.90	0.34	0.42
Co-ZSM5-0.67	1.54	0.67	0.39
Co-ZSM5-0.94	2.15	0.94	0.46
Parent Na-MOR	–	–	0.92
Co-MOR-0.84	3.2	0.84	0.22

2.3. Diffuse reflectance UV–vis spectrophotometry

Diffuse reflectance spectroscopy in the UV–vis region (DRS UV–vis) spectra were obtained in a Cary 5E (Varian) using a high-temperature reaction chamber cell (Harrick Scientific). In all cases, prior to the measurements of the spectra, the samples were dehydrated under the flow of 30 cm^3 N_2/min and under heating at 6 °C/min up to 500°, then the temperature and the N_2 flow were held constants for 30 min to attain complete dehydration of the catalysts. The band at 1905 nm assigned to physisorbed H_2O, was used to track dehydration. The spectral data were acquired with a 0.5-nm resolution. The spectra of the dehydrated parent zeolites were subtracted respectively from those of the catalysts to isolate the Co contributions.

2.4. Temperature-programmed reduction with H_2 (H_2-TPR)

H_2-TPR was used to track the changes in the cobalt before and after catalytic testing under either dry or wet conditions. The characterisation was conducted using 25 mg of catalyst and a flow of 25 cm^3/min of a mixture of 10% H_2 in argon balance through the reactor. The reactor temperature was raised from room temperature at a heating rate of 10 °C/min up to 1000 °C, and the H_2 consumption was measured using a thermal conductivity cell. Prior to the H_2-TPR of the spent catalysts, were dried at 150 °C under N_2 flow for 1.5 h to remove physisorbed H_2O, thereafter the reactor was cooled to room temperature.

3. Results and discussion

3.1. Deactivation of Co-ZSM5 and Co-MOR during SCR-NO_x

The temperature of the reactor was first kept constant at 500 °C and 450 °C for Co-ZSM5 and Co-MOR, respectively, with the dry reaction mixture flowing through the reactor. After 3 h of reaction under these conditions, H_2O was introduced to the feed stream. The introduction of 5% H_2O resulted in an immediate drop in NO_x conversion. This behaviour is apparently caused by competition between the H_2O and NO molecules for cobalt active sites, *i.e.*, kinetic inhibition. This conclusion is based on its reversibility during the first hours of wet operation [3,4]. The catalysts activity is only partially reversible after 12 h of wet operation in the case of Co-ZSM5 catalysts [15], most likely because some structural changes have already occurred. Fig. 1 shows the TOS trajectories of NO_x conversion for both Co-ZSM5 and Co-MOR catalysts with 5% H_2O in the reaction stream. After 80 h of continuous operation, H_2O was removed from the feed to observe the loss in activity caused by the irreversible changes. As seen in Fig. 1, the irreversible deactivation is obvious, as the NO_x conversion did not recover its initial value in dry conditions after H_2O removal, losing 20% and 25% of its initial activity for the Co-ZSM5 and Co-MOR catalysts, respectively.

There are few reports in the literature about the deactivation of zeolite-based catalysts under long-term wet operation at

Table 2
Literature reports of NO_x reduction activity as a function of TOS in the presence of H_2O for zeolite-based catalysts.

Catalyst	Reductant/temperature (°C)	GHSV (h^{-1})	H_2O % (v/v)	Type of curve with TOS	Reference
Co-MFI	i-C_4H_{10}/400	30,000–42,000	10	Pseudo-stationary	[19]
$CoNH_4$-BEA	C_3H_8/350	7500	9	Pseudo-stationary	[30]
Pd/MOR	CH_4/450	15,000	9	Sigmoid-like	[31]
Pd-Co/HMSM5	CH_4/500	~30,000	10	Sigmoid-like	[25]
Fe-ZSM5 and Cu-ZSM5	i-C_4H_{10} and C_3H_8/375 and 400	42,000 and 120,000	10	Linear decrease and parabolic	[32]
Co-MOR	C_4H_{10}/400	20,000	2	Sigmoid-like	[16]
Cu-ZSM5	C_3H_8/400	120,000	10	Sigmoid-like	[53]

isothermal conditions. Some of these studies reported a pseudo-stationary activity, while others reported a sigmoid-like drop in activity (Table 2). For a Co-MFI catalyst, Wang et al. [18] reported a nearly constant N_2 yield using 10% (v/v) of H_2O in the reaction feed, but the CO_2 production followed a sigmoidal path. This suggests that there are changes occurring in the catalysts that are strongly reflected in the hydrocarbon oxidation. The fact that the changes were not reflected in the N_2 yield curve could be due to the low GHSV used in that study (30,000–42,000 h^{-1}), and also in those presented in Table 2, which is less than half of the value used here.

This finding implies that the catalyst operates under less demanding conditions. Čapek et al. [30] also reported quasi-stationary trajectories for $CoNH_4$-BEA catalysts (with 10% H_2O) using a low GHSV of 7500 h^{-1}. Under those experimental conditions, it is difficult to see significant changes in activity during the period used in their study (90 h). Ohtsuka et al. [31] reported for Pd-MOR catalysts a sigmoid deactivation curve (with 9% H_2O) using a GHSV of 15,000 h^{-1}, whereas Ogura et al. [25] reported both a sigmoidal deactivation (10% H_2O) trend and an increase in activity in the initial hours ($t < 5$ h) of operation for Pd-Co/HZSM5 catalysts. Chen et al. [32] reported for Fe-ZSM5 and Cu-ZSM5 that the NO conversion to N_2 followed a parabolic deactivation curve with TOS, particularly in the case of Cu-ZSM5. Recently, Gao et al. [12] reported that Cu/SSZ-13 showed good hydrothermal stability at 400,000 h^{-1}, and even at higher GHSV, however they do not reported a TOS curve.

Although all of the above studies used different metals, reducing agents and operating conditions (Table 2), the presence of H_2O is unambiguously adverse for the stability of zeolite-based catalysts during NO_x reduction. Additionally, the use of high spatial velocities is important for observing the changes in the catalysts because the migration of the metal ions is strongly reflected in the TOS curve, as is the case in Fig. 1.

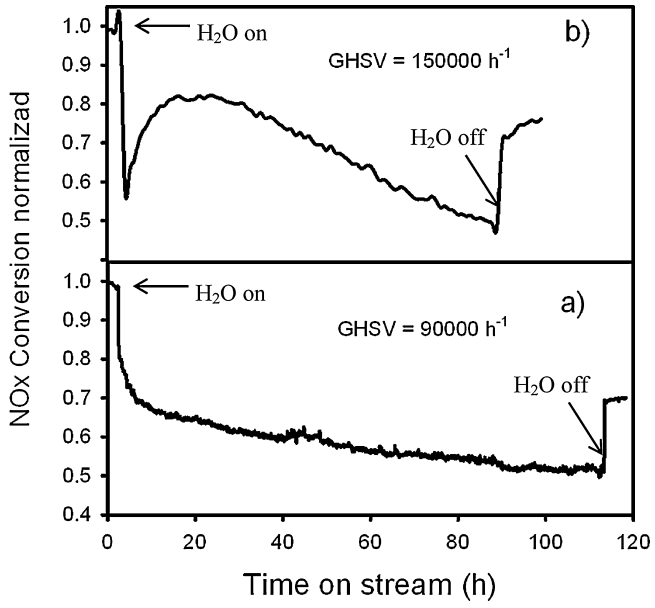

Fig. 1. NO conversion versus time on stream for (a) Co-MOR catalysts ($T = 450$ °C) and (b) Co-ZSM5-0.65 ($T = 500$ °C), both operated with 5% H_2O in the feed reaction stream.

In our previous study [15], we proposed that the initial increase in NO conversion during the wet operation of the Co-ZSM5 catalysts was caused by the rearrangement of Co species leading to an increase in the concentration of active sites (active Co^{2+}). This rearrangement likely occurs through the formation of labile cobalt-hydroxide. At higher TOS, these cobalt-hydroxides condensate first to cobalt-oxyhydroxide species and ultimately to crystallites of Co_xO_y oxide. At the same time, the nucleation process also leads to the relocation of cations towards hard-to-access sites that have lower reactivity for NO_x reduction. The isolation of cations and formation of oxide crystallites has been reported for zeolite-type catalysts deactivated by H_2O, where no destruction of the zeolite matrix occurred [14,15,32].

A theoretical study of the H_2O interaction with the cation exchanged in the zeolite ZSM5 was performed by Rice et al. [33], who found that the adsorption of one H_2O molecule on the cation lengthens the bond between the metal cation and the oxygen atom of the zeolite framework bonded to the cation. This bond becomes weaker as the number of adsorbed H_2O molecules increases, which could explain the enhanced deactivation observed when the concentration of H_2O increases in the reaction mixture. Although their calculations show that metal hydroxide species are less thermodynamically favoured, they indicate that those species can contribute to the redistribution of metal cations in zeolites.

Recent studies have shown that formation of ion/water complex produce deformation of the zeolite framework. Thus constraining the position of the formed complex on the zeolite framework as a function of the net charge of the zeolite. Kwak et al. [9] using Cu/SSZ-13 catalyst showed that in the presence of H_2O there is formation of Cu^{2+} ion/water complexes, and at full hydration the charges of these ions are homogeneously distributed on the zeolite, having as a consequence that the complexes may migrate into the zeolite framework. Their analysis of XRD patterns at different temperatures showed that dehydration of Cu-SSZ-13 caused movements of Cu ions from the large zeolite cages into positions that allow strong interactions with the charge compensation sites of the framework. Gao et al. [12] observed by using EPR, the mobility of Cu^{2+} ions in their Cu/SSZ-13 sample when it was dehydrated, and proposed that H_2O ligands were lost from the first coordination sphere, changing the Cu-dehydrated ions from the 8-membered rings to 6-membered rings of the zeolite. Also they mention that at low metal loading, Cu^{2+} ion monomers are mainly found, whereas at high loadings the Cu dimers are most favoured.

Furthermore, a simulation using forced field, able to model the structure of zeolites, was conducted by Jeffroy et al. [34], who found that there is a correlation between the size of the cation and the variation of the lattice parameters of the zeolites. When the size of the cation decreased the lattice parameters decreased as well. In particular, they found for NaCoX faujasite system that there was a significant deformation of the zeolite framework when the amount of Co atoms was increased in the unit cell (ion exchange) and their

results correlates well with experimental data reported for this zeolite. The variation in the lattice parameters of the zeolite with the hydratation degree of the cation was also observed by Kwak et al. [9] in their Cu-SSZ-13 sample. It seems that the coordination sphere of the hydrated cation should have a key role in the deactivation mechanism caused by the migration of the hydrated cation.

Ahmmad et al. [35] measured the properties of hydrated Co acetate introduced into the pores of SWNT, the formation of a so called "nanosolution" was studied by controlling H_2O adsorption in their samples. They found that the interatomic distance between Co^{2+} and O atoms were shorter in the case of nanosolution compared with the bulk aqueous solution, showing that the coordination or hydration distance depend decisively on the number of coordinated or hydrated atoms, thus a small number of coordinated atoms should give a smaller ionic radius or shorter distance. The latter can explain why the zeolite experience a low deactivation when the reaction stream has low H_2O concentration, because not all the Co ions are fully hydrated, and the size of the coordination sphere of hydrated Co^{2+} ion is small, having as a result less mobility on the zeolite framework, or the apparent stability of the small pore size zeolite compared with the medium pore size zeolite, since in the former case the space constrains restricts the size of the coordination sphere of the cation.

When the amount of H_2O in the reaction stream increases, more Co^{2+} ions can increase the number of water molecules that are coordinated with them. That is, "locally" relax the charge in the compensation charged sites and then the ion/water complex migrates to more stable sites, such as bigger cavities where they acquire more stability. It is plausible that during this transit through the zeolite channels the hydrated ion/complex collide and condense forming dimmers and subsequently MO_x moieties [10,12] with the increase of the time on stream. Vennestrøm et al. [13] showed that the physical mixture of CuO and H-ZSM5 becomes active for NO_x reduction by heating it at 550 °C in presence of NO, NH_3, O_2, H_2O and N_2. Their explanation for this result was that the original proton was exchanged by Cu^{2+} driven by H_2O presence in their reaction stream, which migrates from CuO phase to the ion-exchange position in the zeolite framework, they considered that if CuO is formed during hydrothermal operation in the Cu-zeolite catalysts then the migration of Cu back into compensation charged sites is highly possible. The last is in accordance with our previous report for Co-ZSM5 deactivation during hydrothermal operation [15].

Such as Gao et al. [12] mentioned, the dynamic character of catalytically active centres under wet reaction conditions is the cause for mobility and transient interactions among Cu^{2+} ions, and for that reason is difficult to identify the real nature of catalytic centres. As it could be seen from the current literature, the same observations are applicable for Fe or Co exchanged into the different zeolite types.

We show in the next section that the underlying explanation of our deactivation curves involves the migration and formation of oxide crystallites and isolated cations as a result of interactions with H_2O.

3.2. DRS characterisation

To detect changes in the cobalt species after reaction, we recorded the DR UV-Vis spectra to identify the Co^{2+} species present on the exchange sites of the zeolite structure. The Co^{2+} positioned in the exchange sites of the zeolite shows three *d-d* transition bands, each corresponding to a Co^{2+} ion in a specific site on the zeolite network. Drozdová et al. [27] proposed three Co ion exchange sites, which they labelled α, β and γ. The α site is located in the straight channels of ZSM5 and the main channel of MOR. In ZSM5, the β site is located at the intersection of the straight and

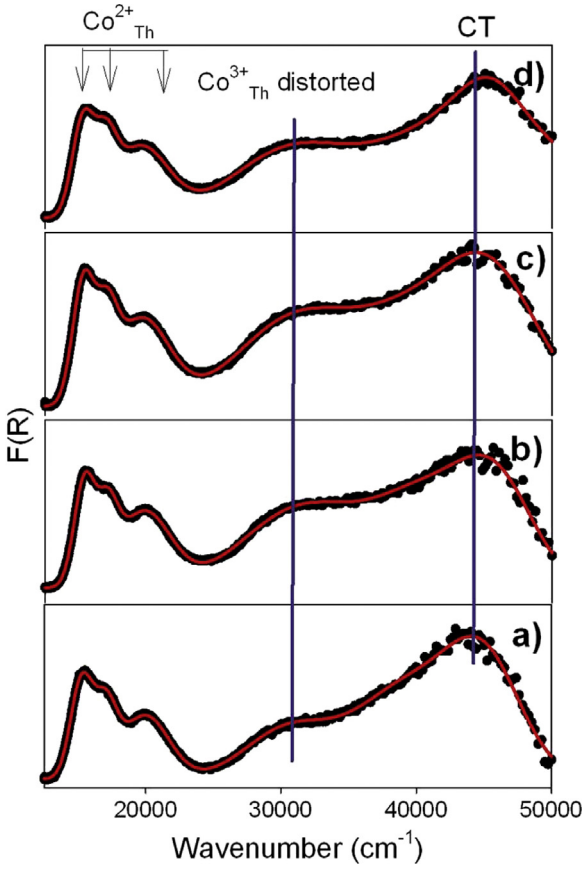

Fig. 2. UV–vis spectra for dehydrated Co-MOR catalyst: (a) fresh catalyst, (b) after 80-h reaction in dry conditions, (c) after 80-h reaction with 5% H_2O in the reaction feed, (d) after 80-h reaction with 10% H_2O in the reaction feed.

sinusoidal channels in the six-member deformed ring, whereas it is located in the twisted eight-membered ring of the MOR cavity in MOR zeolite. The γ sites are located in the "boat-shaped" site of MOR and its equivalent in ZSM5.

The spectra of our catalysts were deconvoluted using only three Gaussian bands because we did not observe other signals when the Co loading was varied over the zeolite, in contrast to the spectra reported by Dědeček et al. [36]. In our analysis of Co-MOR, the α, β and γ sites were associated with the bands centred at 20,202, 17,606 and 15,748 cm^{-1}, respectively.

Fig. 2 shows the spectra of the Co-MOR catalyst treated under different reaction conditions. In the spectrum of all samples, the bands corresponding to the tetrahedral Co^{2+} ion can be observed, as well as a band at approximately 30,926 cm^{-1} assigned to Co^{3+} tetrahedral and Co^{2+} octahedral distorted environment [37,38] and a band centred at 44,100 cm^{-1} assigned to metal–ligand charge transfer (CT). The band at 30,926 cm^{-1} indicates that not all of the Co was positioned in the compensation charge sites of the zeolite. This band increased after the solid was used in the reaction, suggesting that a fraction of original exchanged metal turned into CoO_x species.

To detect changes in the Co^{2+} isolated species after reaction under dry and wet conditions, NO was adsorbed at room temperature after catalyst dehydration. As seen in Fig. 3 for Co-MOR catalysts, the triplet assigned to the isolated Co^{2+} is almost suppressed after NO adsorption when the catalyst has not been used in reaction (fresh solid, Fig. 3a): The same is observed in the spectrum of the catalyst used for 80 h under dry conditions (Fig. 3b). As the catalysts are deactivated under reaction stream (see Fig. 2), the Co^{2+} bands show a noticeable intensity after NO

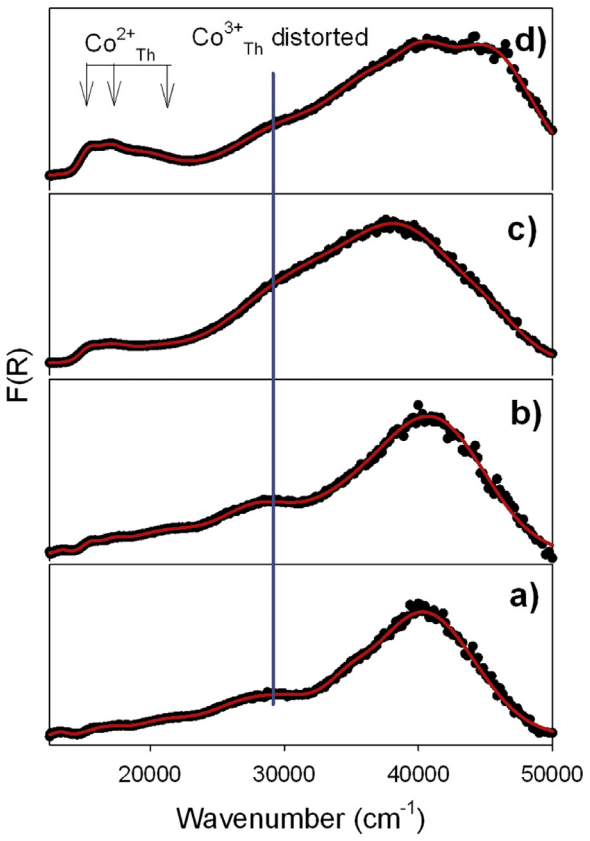

Fig. 3. UV–vis spectra for Co-MOR catalyst after NO adsorption in situ at room temperature: (a) fresh catalyst, (b) after 80-h reaction in dry conditions, (c) after 80-h reaction with 5% H_2O in the reaction feed, (d) after 80-h reaction with 10% H_2O in the reaction feed.

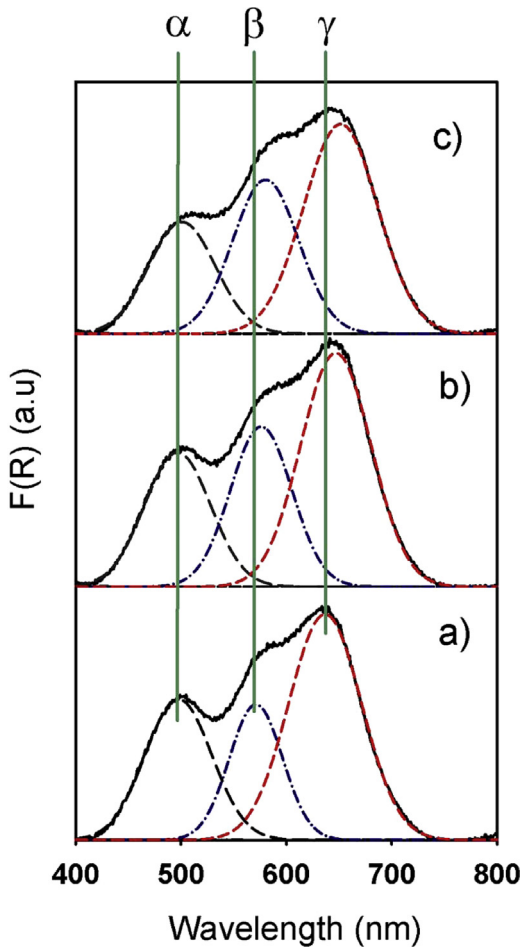

Fig. 4. UV–vis spectra of Co-MOR catalysts: (a) calcined-only catalyst, (b) after reaction in dry conditions, (c) after reaction with 10% (v/v) H_2O in the reactor feed.

is adsorbed, meaning that not all cations are able to interact with the NO molecules. This has also been observed in deactivated zeolite-based catalysts by experiments using the temperature-programmed desorption of NO, where a decrease in the NO_x storage capacity is observed [e.g., 39]. Another important feature of the UV-vis spectra of the Co-MOR solids with adsorbed NO is the red-shift of the maximum of the CT band. This red-shift of the CT band was also observed by Klier et al. [40] when they adsorbed NO on Co-erionite; however, in their study, they did not provide an explanation of this behaviour. Furthermore, in addition to the red-shift of the CT band, a signal at 44,100 cm^{-1} is also present in the case of the catalyst deactivated with 10% H_2O in the reaction stream (Fig. 3d). The presence of these two CT bands suggests that the band shift may be attributed to active Co^{2+} sites, whereas the band that remains unchanged could be associated with non-active Co^{2+} sites that are not available for NO adsorption.

Fig. 4 shows the UV–vis spectra of the Co-MOR catalysts before and after reaction. A red-shift was observed for the bands assigned to β and γ Co sites, which was more evident when the catalyst was severely deactivated (spectra c in Fig. 2) This shift may be associated with changes in the position of the β and γ cations during the deactivation process, when they acquire a different spatial configuration inside the zeolite framework as a result of the weakening of the bond between the T-O sites of the zeolite and the cations (as discussed above) during deactivation.

In the case of the Co-ZSM5 catalysts, the α, β and γ sites were associated with the bands centred at 20,040, 17,271 and 15,456 cm^{-1}, respectively. The Co^{3+} in a distorted tetrahedral environment was assigned to the band centred at 28,785–29,425 cm^{-1}. The CT band was observed at 48,230 cm^{-1}; unlike in the Co-MOR catalysts, it does not show a significant shift to low energy with NO adsorption (Fig. 5). The DR UV–vis spectra of our catalysts reveal the presence of Co^{2+} in a tetrahedral environment as well as a band assigned to Co^{3+} distorted tetrahedral for the fresh solids, meaning that not all of the Co was positioned in the compensation charge sites of the zeolite during the ion exchange process. When NO was adsorbed on fresh and deactivated catalysts, the spectra of the latter showed bands assigned to the Co^{2+}, indicating that a fraction of the existing Co^{2+} ions cannot adsorb NO (Figs. 5c and 6c).

A peculiar effect of NO adsorption over Co-ZSM5 solids is that in the fresh samples, the band assigned to the Co^{2+} ions in the β position did not disappear completely, which suggests that this position in the zeolite framework makes the ions less accessible to NO molecules.

In the case of Co-ZSM5-0.34 (Fig. 5), a small band around 40,000 cm^{-1} is present in the fresh solid. This band remained when the NO was adsorbed and disappeared once the catalyst was deactivated. The Co-ZSM5-0.94 (Fig. 6) catalyst showed also broad band at 40,000 cm^{-1} corresponding to the CT band when NO is adsorbed on the fresh solid; the broad band observed in this case could be related to a high metal loading on this catalyst. However, the band at 40,000 cm^{-1} disappeared in the deep deactivated catalyst, as also occurred in the case of Co-ZSM5-0.34.

For the Co-ZSM5 deeply deactivated catalysts, no significant changes were observed in the position of the maximum of the bands associated with the α, β or γ sites (not shown). In contrast, the Co-MOR catalysts exhibited a red-shift of the bands assigned to the β and γ sites. This reveals the difficulty in observing the cation position changes in ZSM5 zeolite after irreversible deactivation.

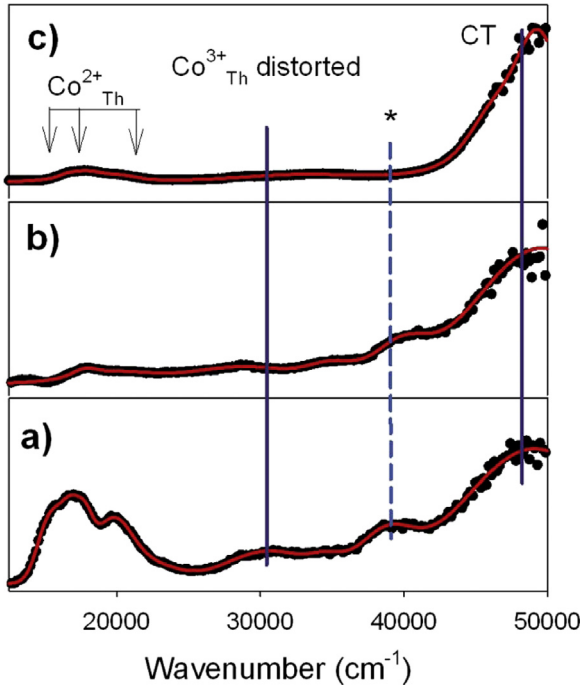

Fig. 5. UV–vis spectra of Co-ZSM5-0.34: (a) fresh catalyst, (b) fresh catalyst with NO adsorption in situ at room temperature, (c) deactivated catalysts with NO adsorption in situ at room temperature.

3.2.1. H_2-TPR

To observe the changes in the species present in the catalysts before and after reaction, the H_2-TPR characterisation of the dehydrated solid and in situ after deactivation was performed. Based on our previous results [15] and the literature [9,10,41,42], we assigned the reduction of the Co species as follows for ZSM5:

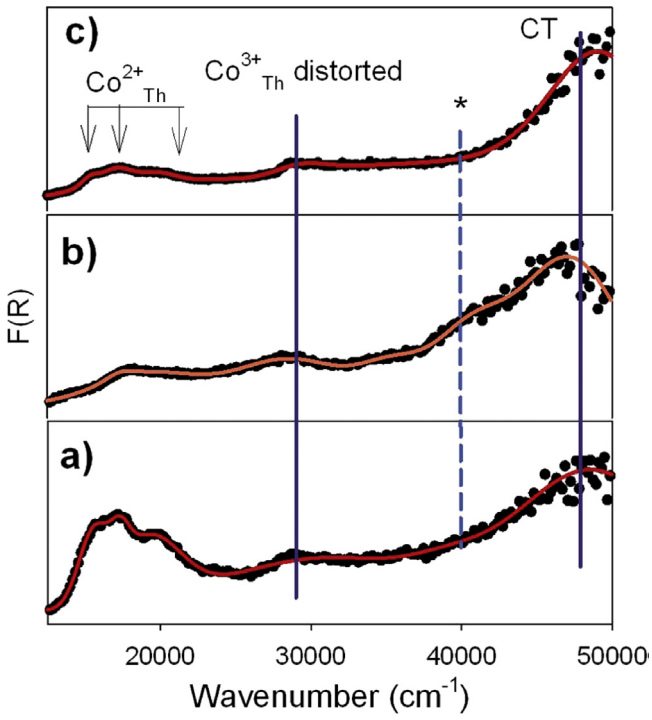

Fig. 6. UV–vis spectra of Co-ZSM5-0.94: (a) fresh catalyst, (b) fresh catalyst with in situ NO adsorption at room temperature, (c) deactivated catalysts with in situ NO adsorption at room temperature.

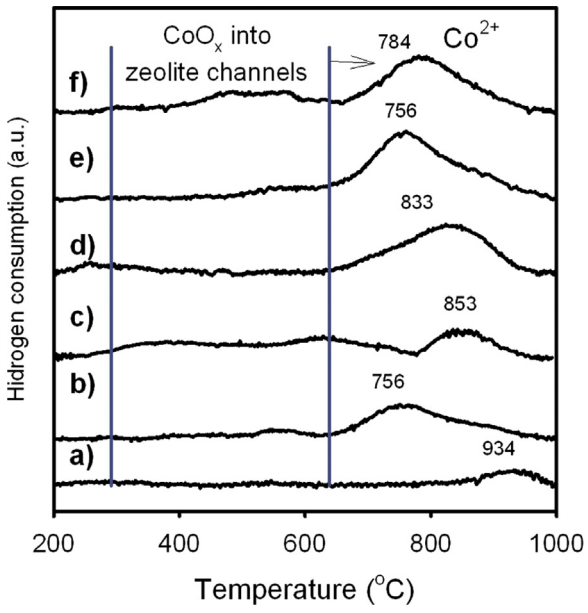

Fig. 7. H_2-TPR profiles of Co-ZSM5-0.34 catalyst: (a) fresh, (b) treated at 500 °C with a wet air stream (33% H_2O) for 17 h, (c) after deactivation during NO_x reduction reaction with 10% H_2O (reaction time of 80 h). H_2-TPR profiles of Co-ZSM5-0.65 catalyst: (d) fresh solid, (e) treated at 500 °C with a wet air stream (33% H_2O) for 17 h, (f) after deactivation during NO_x reduction reaction with 10% H_2O (reaction time of 80 h).

100–350 °C: Reduction of highly dispersed Co_3O_4 crystallites located outside of the zeolite pore structure and reduction of oxocations $[Co–O–Co]^{2+}$.
350–600 °C: Reduction of CoO_x stabilised inside the zeolite channels.
600–1000 °C: Reduction of isolated Co^{2+} bound to exchange sites of the zeolite.

For Co-MOR, it has been reported that two signals are observed due to reduction of Co^{2+} ions [43] as well as the oxide species.

At $T < 600$ °C: Reduction of highly dispersed Co_3O_4 crystallites located outside of the zeolite pore structure and reduction of oxocations.
650–710 °C: Reduction of Co^{2+} situated in the exchange sites of 12-member ring channels.
850–900 °C: Reduction of Co^{2+} ions situated in the exchange positions in the side pockets.

It was previously observed that, in the fresh Co-ZSM5 catalysts, the peak associated with Co^{2+} reduction appeared at higher temperature as the cobalt loading in the catalyst decreased. When we introduced H_2O to study the changes in the catalysts due solely to the presence of this compound in a wet air stream, the maximum of the Co^{2+} reduction peak was located at nearly the same temperature, i.e., a similar Co^{2+} distribution was reached as a result of the hydrothermal treatment [15]. Additionally, only small peaks corresponding to oxide-like compounds were observed with this hydrothermal treatment (Figs. 7b and 9e).

On the other hand, for long-term reaction under wet operation (TOS > 12 h), all of the deeply deactivated catalysts exhibited reduction peaks in the 350–600 °C range (Fig. 7), which is consistent with the coarsening of the oxide crystallites formed during the deactivation process. Furthermore, the Co^{2+} reduction peak also shifted to high temperature, implying that a significant fraction of these ions became refractory against reduction and consequently less active in the reduction of NO_x.

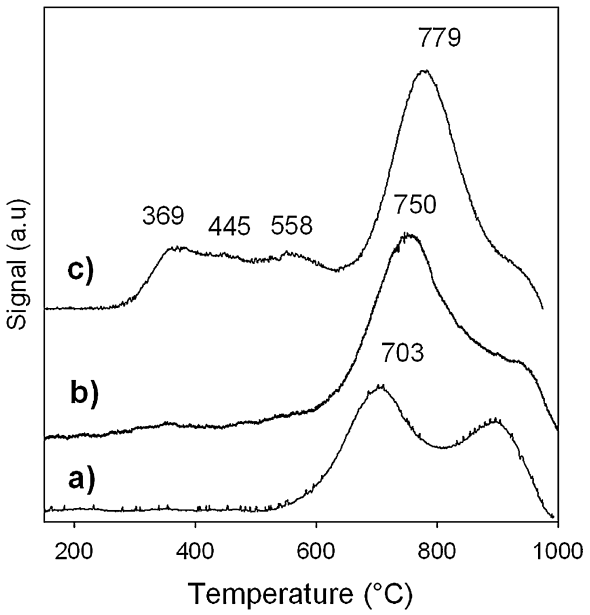

Fig. 8. H_2-TPR profiles of Co-MOR catalyst: (a) fresh, (b) treated at 500 °C with a wet air stream (33% H_2O) for 80 h, and (c) after deactivation during NO_x reduction reaction with 10% H_2O (reaction time of 80 h).

In the case of Co-MOR catalysts, when solely H_2O was introduced in a wet air stream, a general decrease in the intensity of the high-temperature peak was observed, which is associated with the reduction of Co^{2+} into the side pockets, as well as a small peak at approximately 370 °C (Fig. 8b). When the catalysts underwent deep deactivation during reaction wet operation, three peaks were found in the H_2-TPR pattern (Fig. 8c), which are associated with the CoO_x inside the zeolite channels [43], indicating a coarsening of the cobalt to form oxide-like compounds, as is also observed in Co-ZSM5.

Additionally, for this catalyst, a shift to high temperature for the reduction of the Co^{2+} peak (located in the 12-member ring channels) was observed when irreversible deactivation occurred. Our results for both cobalt-zeolite-based catalysts suggest that the irreversible deactivation promoted by H_2O during NO_x reduction reaction involves both the agglomeration of cobalt in oxide-like compounds and the isolation of the Co^{2+} located in charged compensation sites inside of the zeolites.

3.3. Kinetics of deactivation

Our discussion of the possible metal rearrangements suggests that deactivation in the presence of H_2O could be envisaged to follow a cation-migration plus nucleation pathway. In the case of the zeolite catalysts studied, there is an initial fast decay, which can be associated with Co migration leading to the formation of CoO_x species. This formation occurs in parallel with the isolation of Co^{2+} sites into the zeolite compensation charged sites. The migration of cations is evidenced by the fact that, at the end of the catalytic test, a fraction of the Co species became refractory against reduction by H_2 and presumably less active for NO reduction. Furthermore, DR UV-vis spectroscopy revealed that a fraction of the Co^{2+} sites became less accessible to NO adsorption. Vennestrøm et al. [13], observed also an isolation of Cu ions on Cu-zeolite catalysts, and suggested that $[Cu(OH)]^+$ species formed by the hydration of Cu^{2+} can form dimers by migration, only in the case of having a closer neighbouring site, otherwise these species remain as isolated ions.

A scheme of the deactivation process is given in Fig. 9. The irreversible deactivation stages could be visualised as migrations

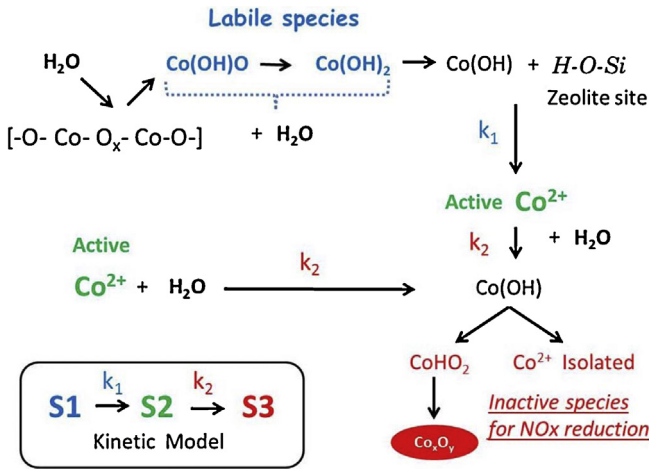

Fig. 9. Scheme proposed for the irreversible deactivation of Co-ZSM5 and Co-MOR catalysts during reaction under wet operation at $T \leq 500$ °C and the kinetic model proposed for the development of inactive Co sites.

of ion/water complex that are detached from the compensation charged sites and forms oxyhydroxide species by condensation of two or more hydrated ions [15]. Further migrations lead these to form crystallites of metal oxide, likely by interactions between Co sites located in close proximity to each other. This phenomenon constitutes one cause of irreversible deactivation. The second cause corresponds to the isolation of Co^{2+} cations in zeolite sites in where they acquire more stability and hence less reactivity for the NO_x reduction reaction. Several studies have found that metal cations can remain as isolated species even when the catalysts undergo severe deactivation even when there is no dealumination of the zeolite [14,15,44].

Additionally, our H_2-TPR and UV-vis spectra with NO adsorption indicated that the coarsening of cobalt sites is evident only in the reaction atmosphere, meaning that the kinetics of this process is accelerated by the H_2O, just as when the reaction occurs over the catalyst. This observation is also in accordance with the sintering and re-dispersion of metals over several catalysts [45].

We modelled this phenomenon using the design equation for a packed bed reactor (PBR):

$$\frac{W}{F_{NOo}} = \int_{X_{max}}^{X_s} \frac{dX_{NO}}{-r_{NO}} \quad (1)$$

where W is the catalyst weight, F_{NOo} is the initial molar flow of NO in the reaction feed, $-r_{NO}$ is the NO reaction rate, X_{max} is the maximum NO_x conversion reached during reaction in wet conditions and X_s is the stationary conversion reached after full deactivation measured in wet conditions (Fig. 1). The following assumptions were made [46]: (i) the deactivation process is only due to changes in the catalytic solid, meaning that the concentration of the reacting or product compounds has no effect; (ii) because the concentration of reacting compounds in the reaction mixture is small, we considered the change in the gas volume to be negligible; (iii) the excess C_3H_8 in the reaction mixture creates pseudo-first-order kinetics with regard to the NO compound ($-r_{NO} = kC_{NO}$). The values of k obtained (see Tables 3 and 4) are in the range of those reported by other authors for this type of catalyst for NO_x reduction with excess ammonia [47].

Furthermore, to model the change in the metal species in the catalyst, we propose that the cobalt species could be classified into three categories and that the changes between them could be related by pseudo-first-order reactions in series. These reactions occur as $S_1 \xrightarrow{k_1} S_2 \xrightarrow{k_2} S_3$, where S_1 is the cobalt site that could turn to an active site S_2 (as observed in the Co-ZSM5 TOS deactivation

Table 3
Parameters of Eq. (4) obtained by the fitting of the curves for Co-ZSM5 wet deactivation (Fig. 10).

Parameter	Co-ZSM5-0.34		Co-ZSM5-0.67		Co-ZSM5-0.94	
	Value	Std. Error	Value	Std. Error	Value	Std. Error
k (cm^3/g^*s)	43.2	–	83.6	–	89.6	–
k_d (Al_{atom}^{-1})	4.125E−19	1.515E−20	7.621E−20	8.704E−21	4.027E−20	5.196E−21
k_1 (s^{-1})	1.624E−5	8.767E−7	5.592E−6	6.446E−7	4.195E−6	4.270E−7
k_2 (s^{-1})	4.277E−5	3.884E−6	2.668E−5	1.741E−6	4.540E−5	2.180E−6
M	6.942	0.968	13.627	1.217	27.648	1.941
X_s	0.183	0.004	0.205	0.032	0.301	0.025

Table 4
Values for the parameter of equation 4 obtained by the fitting of the curves for Co-MOR-0.84 dry and wet deactivation (Fig. 11).

Parameter	Dry reaction		5% H_2O		10% H_2O	
	Value	Std. Error	Value	Std. Error	Value	Std. Error
k [cm^3/g^*s]	91.6	–	78.2	–	68.3	–
k_d (Al_{atom}^{-1})	1.261E−19	2.033E−21	4.306E−20	5.515E−22	3.833E−20	4.777E−22
k_1 (s^{-1})	1.082E−5	1.280E−7	3.518E−6	1.258E−7	7.088E−6	9.638E−8
k_2 (s^{-1})	8.486E−5	2.524E−6	1.150E−4	3.497E−6	2.444E−4	8.479E−6
M	3.271	0.067	16.363	0.580	16.674	0.451
X_s	0.904	3.764E−4	0.433	0.006	0.297	0.001

patterns), which is then converted to an inactive cobalt site S_3 (Fig. 9). The changes in the concentration of S_2 sites are related to the TOS (solving the kinetic model) by Eq. (2):

$$f_{S_2}(t) = \frac{C_{S_2}(t)}{C_{S_2 o}} = \frac{k_1 M}{k_2 - k_1}(e^{-k_1 t} - e^{-k_2 t}) + e^{-k_2 t} \quad (2)$$

The factor M is the ratio between the initial concentrations of both S_1 ($C_{S_1 o}$) and S_2 sites ($C_{S_2 o}$), and it was considered that $C_{S_2} = C_{S_2 o}$ at the beginning of wet reaction after H_2O inhibition (i.e., this point was taken as $t = 0$). The factor M then could be related with the mobility or degree of rearrangement of the Co^{2+} site before it turns into inactive specie.

The loss of catalytic activity (a) is in essence directly proportional to the fraction of active sites S_2 and the total amount of cobalt atoms ([Co_{at}]) present in the catalyst: $a(t) \propto f_2(t)$ [Co_{at}]. If we use the amount of Al atoms in the zeolite catalysts, and supposing that all cobalt atoms in the zeolite are located on the charge compensation sites (i.e., [Co_{at}] = [Co^{2+}]), Eq. (3) describes the activity decay:

$$a(t) = k_d N_{Al} \phi \cdot f_{S_2}(t) \quad \text{with} \quad \phi = \left(\frac{[Co^{2+}]_o}{N_{Al}} \right) \quad (3)$$

where k_d is a constant of proportionality and is equal in our case to the deactivation constant, N_{Al} is the total amount of aluminium atoms in the zeolite, ϕ is the ion exchange ratio reported in Table 1 as Co^{2+}/Al, and $f_{S_2}(t)$ is the fraction of S_2 sites as a function of the reaction time (Eq. (2)). Eq. (1) was integrated and combining Eqs. (1)–(3), with a rearrangement of the terms, results in Eq. (4). In our case, the use of X_{max} equal to one instead of the experimental maximum of the deactivation curves gave a better fit of the model to the deactivation data.

$$X(t) = (1 - X_s)\left(1 - e^{\left\{-\tau k \left[(k_d N_{Al}\phi)\left((k_1 M/k_2 - k_1)(e^{-k_1 t} - e^{-k_2 t}) + e^{-k_2 t}\right)\right]\right\}}\right) + X_s \quad (4)$$

where $X(t)$ is the NO_x conversion as a function of TOS, τ is the spatial time of the reactor and X_s is the stationary conversion reached in wet conditions by the deactivated catalysts.

3.4. Fit of deactivation curves with the deactivation model

For the Co-ZSM5 catalyst, a sigmoidal deactivation pattern was observed after the activity reached its maximum value in the presence of H_2O, after which a slow decrease was observed with respect to the TOS. It was found that Eq. (4) fits the deactivation data very well in the three cases shown. The beginning of the deactivation fit was chosen as the point at which the drop in NO_x conversion stops (due to H_2O introduction), as is shown in Figs. 10 and 11 with an oval. The fit for the Co-ZSM5 catalysts is shown in Fig. 10, and the values for the parameters of Eq. (4) obtained from the regression are given in Table 3.

From Table 3, it can be observed that k_1 is higher for the Co-ZSM5-0.34 catalyst than the other two solids and decreases as the metal loading increases. These values of k_1 suggest that S_1 sites could be transformed into S_2 sites quickly in the low-metal-loading catalyst. This may happen if there are compensation charge sites on the zeolite not bonded to cobalt ions, as is expected in the low-metal-loading catalyst. This allowed the rapid migration of cobalt ions towards these unbonded zeolite sites, thus forming new S_2 sites. The proton sites on the zeolite may prompt the migration process, which could explain why proton-exchanged zeolites are less stable in wet streams than metal-exchanged zeolites are [e.g., 13,48]. Jeffroy et al. [28] found via molecular simulations that when cobalt and sodium were present in the zeolite as exchanged cations, only in the case of cobalt there were movements of their hydrated ion into the X faujasite framework, as the sodium cation does not interacted strongly with water. That could explain why sodium exchanged zeolites have more resistance towards hydrolysis reaction than the proton-exchanged zeolites.

Furthermore, k_2 is almost the same for low- and high-metal-loading catalysts, suggesting that both solids can form either inactive cobalt ions or oxide-like crystallites (both envisaged as S_3 sites) at the same kinetic rate. However, the loss in activity by the formation of S_3 sites is less marked in the high-metal-loading catalysts. This could be rationalised by the presence of oxo-cations or oxide-like species in the ion-exchanged zeolites [49,50], which can migrate by forming oxyhydroxide species via reactions with H_2O present in the reaction stream. If we consider such migrations of oxyhydroxide species as "random" relocations, there is a high probability that successive migrations of these species could liberate a cobalt atom, as was observed for CuO and H-zeolite catalysts [13] and develop an S_1 site, with the possibility of forming an S_2 site afterwards. Therefore, the migration of these oxyhydroxide species serves as a reservoir of S_2 active sites, which gradually replaces the loss of those S_2 sites that are transformed in parallel migrations to S_3 sites; in this way, the irreversible deactivation process is less

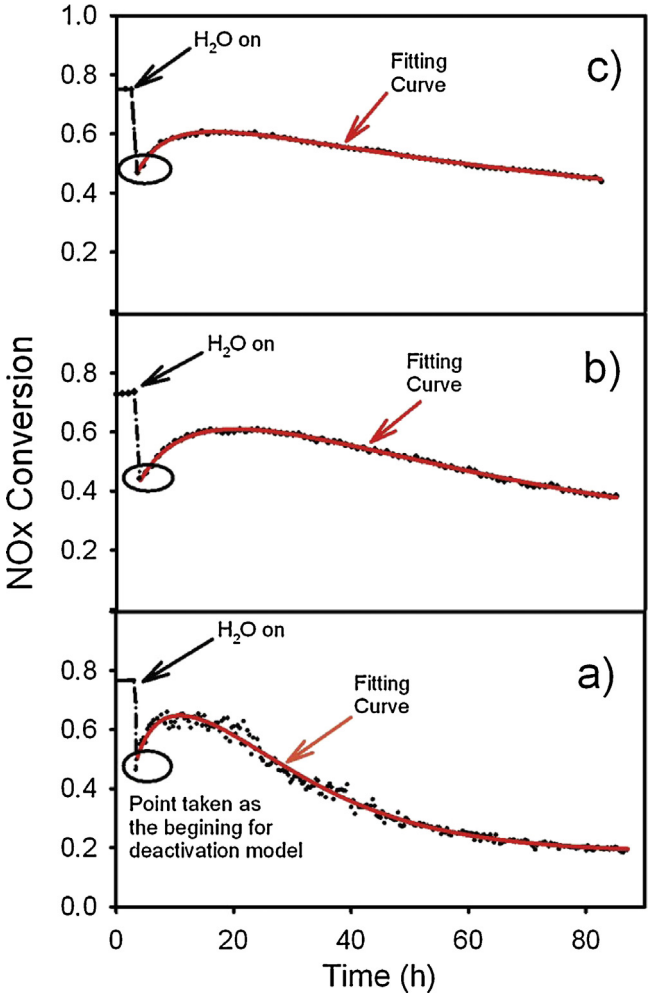

Fig. 10. Fit of the deactivation patterns with Eq. (4) for Co-ZSM5 catalysts during reaction with 10% H_2O in the feedstream at $T = 500\,^{\circ}C$: (a) Co-ZSM5-0.34, (b) Co-ZSM5-0.67, (c) Co-ZSM5-0.94.

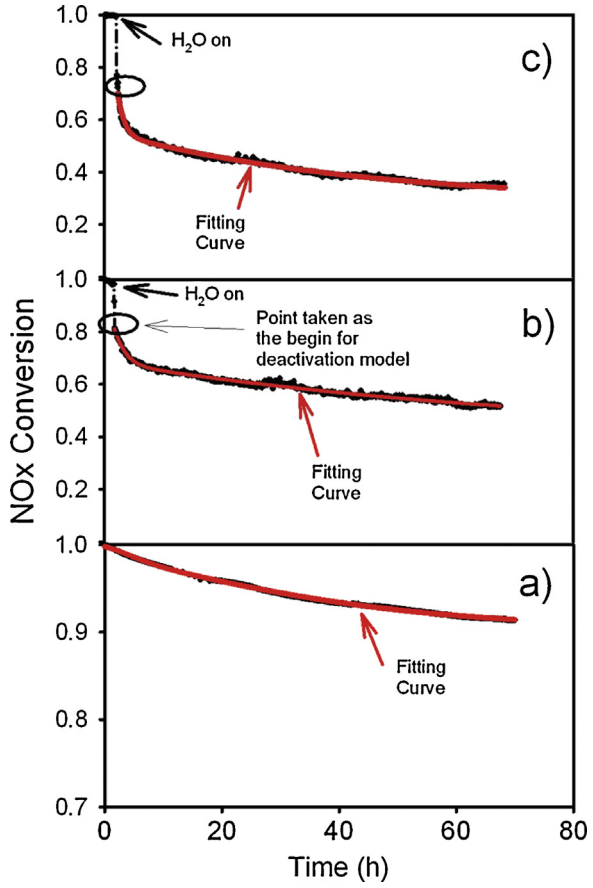

Fig. 11. Fit of the deactivation patterns with Eq. (4) for Co-MOR catalyst with and without H_2O in the feedstream during reaction at 450 °C: (a) 0% H_2O, (b) 5% H_2O, (c) 10% H_2O.

evident in high-metal-loading catalysts. The values of the M factor in Table 3 are in accordance with the idea of the relocations of Co ions, with the amount of potential S_1 sites that can be transformed to S_2 being highest for the high-metal-loading catalyst and thereby damping the deactivation process. The last is also in line with the values of k_d (deactivation constant) obtained because the values show that the extent of irreversible deactivation increases as the metal loading in the catalyst decreases, which is in agreement with our experimental results and other reports as well [51,52].

Our kinetic results are in agreement with the theoretical and experimental results of several authors [9,12,28,33], who found that a large concentration of H_2O molecules weakens the bond between Co^{2+} sites and zeolite charge compensation sites because of the increased Co^{2+}-H_2O interactions. It should be expected that with the same concentration of H_2O in the reactor feed, the deactivation process would be slower in catalysts with high metal loading.

Co-MOR catalysts experienced a different deactivation pattern than the Co-ZSM5 catalysts. The activity of these catalysts decayed exponentially in the first hours, followed by a slow decrease with respect to the TOS, as has been observed in other studies [e.g., 16,24,26]. For this catalyst, the kinetic inhibition upon the reaction constant (k) due to the presence of H_2O in the reaction feed was estimated by means of the expression $k_{inh} = k(1/1 + b[H_2O])$, where k_{inh} is the kinetic constant observed according to the amount of H_2O in the reaction stream and b is a constant. Fig. 11 shows the fit for the deactivation data of this catalyst using Eq. (4), and the values obtained from the regression are given in Table 4.

Fig. 11 shows that the model fits the decay of NO_x conversion during deactivation well. The values of k_2 in Table 4 reinforce the assumption that a high concentration of H_2O in the reactor feed promotes the migration of cobalt species (towards S_3 sites) because the Co^{2+}-zeolite bond is weakened by H_2O; this weakening increased as the water content in the reaction feed increased, as discussed above.

As observed from the comparison of k_1 values for both types of zeolite catalysts, Co-MOR presented the low values of k_1 and the highest values of k_2. This suggests that the Co species in MOR zeolite migrates as a result of the presence of H_2O without forming active S_2 sites in the process, and the weakening of Co^{2+}-zeolite bonds then leads to the rapid formation of oxide-like compounds and the isolation of ions in zeolite locations, where they are not accessible to NO_x reduction reaction. It has been reported in the case of the use of zeolites as catalyst support for NO_x reduction reaction that there is a large migration of cobalt cations to locations inside the channels, where the cations become isolated and stable against reacting molecules [14,15]. It is not yet completely understood why the deactivating effect of H_2O during NO_x reduction is higher for MOR zeolite than ZSM5, however a possible explanation can be found in the pore size and effective volume of MOR zeolite compared with the ZSM5 zeolite [29]. The formed Co^{2+}/water complex may move with fewer restrictions in the case of MOR zeolite due to its larger accessible volume. Furthermore, the differences in the Si/Al ratio cannot be discarded as a probable cause, thus

more studies should be conducted to clarify the key steps of this behaviour.

As seen in Figs. 10 and 11, a larger ratio of $[H_2O]/[Co^{2+}]$ (concentration of H_2O/concentration of Co^{2+}) increased the extent of irreversible deactivation of both zeolite-based catalysts. Moreover, the low X_s value resulting from the increased amount of H_2O in the reactor feed indicates that the catalyst undergoes a more extensive irreversible deactivation. It is usually found that NO_x conversion slows to 20 or 30% during wet operation, and zero-value conversion is not observed, even after deep catalyst deactivation [15,53]. The residual activity most likely results from a fraction of the still-active cations [10,13] coupled with the contribution of Brønsted sites on the zeolite, which could explain the observed value of X_s for both Co-ZSM5-0.34 and Co-MOR-10% H_2O deactivated catalysts.

Our results and the use of Eq. (4) indicates that if the catalytic test is performed at high spatial velocities at the temperature of the maximum NO_x conversion, the migration of active cations into the zeolite matrix can be accelerated, as observed in the results presented in Table 2, all in the absence of zeolite dealumination.

Nevertheless, more effort should be directed towards determining the nature of this phenomenon and understanding the proper form of the proposed S_1, S_2 and S_3 sites and how the zeolite topology affects the metal migration under wet reaction conditions.

4. Conclusions

The deactivation of Co-zeolite deNO_x catalysts promoted by H_2O can be represented by a deactivation model, in which small crystallites of cobalt oxide, as well as isolated ions, are formed. The isolation of the cations in our deactivated catalysts was evident from the DR UV–Vis spectra where the three *d-d* transition bands characteristic of Co^{2+} cations are clearly observed. The deactivation process was modelled successfully using the packed bed reactor design equation and a series of reactions added to the reactor equation. More work is needed to separate the interdependent effects of Co loading (or degree of ion exchange) and H_2O concentration in the reactor feed on the deactivation process.

Acknowledgments

This work was supported by grants from Consejo Nacional de Ciencia y Tecnología-México (CONACYT) (projects 400200-5-38049U and 400200-5-29272U) and Universidad A. Metropolitana-Iztapalapa (UAM-1250203). We would like to thank Prof. A. Boix (UNL) for discussions about the results.

References

[1] M. Iwamoto, H. Yahiro, Y. Yuu, S. Shundo, N. Mizuno, Shokubai 32 (1990) 430.
[2] M. Iwamoto, H. Hamada, Catal. Today 10 (1991) 57.
[3] Y. Li, J.N. Armor, Appl. Catal. B 1 (1992) L31.
[4] Y. Li, P.J. Battavio, J.A. Armor, J. Catal. 142 (1993) 561.
[5] J.N. Armor, T.S. Farris, Appl. Catal. B 4 (1994) L11.
[6] M.D. Fokema, J.Y. Ying, Catal. Rev. 43 (1–2) (2001) 1.
[7] A. Fritz, V. Pitchon, Appl. Catal. B 13 (1997) 1.
[8] P.G. Blakeman, E.M. Burkholder, H.-Y. Chen, J.E. Collier, J.M. Fedeyko, H. Jobson, R.R. Rajaram, Catal. Today 231 (2014) 56.
[9] J.H. Kwak, T. Varga, C.H.F. Peden, F. Gao, J.C. Hanson, J. Szanyi, J. Catal. 314 (2014) 83.
[10] S. Brandenberger, O. Kröcher, M. Casapu, A. Tissler, R. Althoff, Appl. Catal. B: Environ. 101 (2011) 649.
[11] S. Shwan, J. Jansson, E.C. Adams, M. Skoglundh, Catal. Lett. 143 (2013) 43.
[12] F. Gao, E.D. Walter, M. Kollar, Y. Wang, J. Szanyi, C.H.F. Peden, J. Catal. 319 (2014) 1.
[13] P.N.R. Vennestrøm, T.V.W. Janssens, A. Kustov, M. Grill, A. Puig-Molina, L.F. Lundegaard, R.R. Tiruvalam, P. Concepción, A. Corma, J. Catal. 309 (2014) 477.
[14] S.A. Gómez, A. Campero, A. Martínez-Hernández, G.A. Fuentes, Appl. Catal. A 197 (2000) 157.
[15] A. Martínez-Hernández, G.A. Fuentes, Appl. Catal. B: Environ. 57 (2005) 167.
[16] A.V. Boix, S.G. Aspromonte, E.E. Miro, Appl. Catal. A 341 (2008) 26.
[17] P. Ciambelli, D. Sannino, E. Palo, A. Ruggiero, Topics Catal. 42–43 (2007) 177.
[18] X. Wang, H.-Y. Chen, W.M.H. Sachtler, Appl. Catal. B 26 (2000) L227.
[19] X. Wang, H.-Y. Chen, W.M.H. Sachtler, Appl. Catal. B 29 (2001) 47.
[20] D. Kaucký, A. Vondrová, J. Dědeček, B. Wichterlová, J. Catal. 194 (2000) 318.
[21] J. Janas, W. Rojek, S. Dzwigaj, Catal. Today 191 (2012) 32.
[22] L. Čapek, J. Dědeček, B. Wichterlová, J. Catal. 227 (2004) 352.
[23] J.A.Z. Pieterse, R.W. Van den Brink, S. Booneveld, F.A. De Bruijn, Appl. Catal. B 39 (2002) 167.
[24] J.A.Z. Pieterse, R.W. Van den Brink, S. Booneveld, F.A. De Bruijn, Appl. Catal. B 46 (2003) 239.
[25] M. Ogura, S. Kage, T. Shimojo, J. Oba, M. Hayashi, M. Matsukata, E. Kikuchi, J. Catal. 211 (2002) 75.
[26] L.F. Córdoba, G.A. Fuentes, C. Montes de Correa, Micropor. Mesopor. Mater. 77 (2005) 193.
[27] L. Drozdová, R. Prins, J. Dědeček, Z. Sobalík, B. Wichterlova, J. Phys. Chem. B 106 (2002) 2240.
[28] M. Jeffroy, E. Borissenko, A. Boutin, A. Di Lella, F. Porcher, M. Souhassou, C. Lecomte, A.H. Fuchs, Micropor. Mesopor. Mater. 138 (2011) 45.
[29] Ch. Baerlocher, L.B. McCusker, Database of Zeolite Structures: http://www.iza-structure.org/databases/
[30] L. Čapek, J. Dědeček, B. Wichterlova, J. Catal. 227 (2004) 352.
[31] H. Ohtsuka, T. Tabata, T. Hirano, Appl. Catal. B 28 (2000) L73.
[32] H.-Y. Chen, W.M.H. Sachtler, Catal. Today 42 (1998) 73.
[33] M.J. Rice, A.K. Chakraborty, A.T. Bell, J. Phys. Chem. A 102 (1998) 7498.
[34] M. Jeffroy, C.N. -Draghi, A. Boutin, Mol. Simul. 40 (1–3) (2014) 6.
[35] B. Ahmmad, M. Nishi, F. Hirose, T. Ohkubo, Y. Kuroda, Phys. Chem. Chem. Phys. 15 (2013) 8264.
[36] J. Dědeček, L. Čapek, D. Kauchý, Z. Sobalík, B. Wichterlová, J. Catal. 211 (2002) 198.
[37] S. Lim, D. Ciuparu, C. Pak, F. Dobek, Y. Chen, D. Harding, L. Pfefferle, G. Haller, J. Phys. Chem. B 107 (2003) 11048.
[38] F.E. Triguero, C.M. Ferreira, J.C. Volta, W.A. Gonzales, P.G. Pries de Oliveria, Catal. Today 118 (2006) 425.
[39] H. Tounsi, S. Djemel, A. Ghorbel, G. Delahay, L. Charles de Menorval, B. Coq, React. Kinet. Catal. Lett. 81 (1) (2004) 33.
[40] Klier K., Herman R.G., Dědeček J., "NO decomposition in non-reducing atmospheres", Technical Progress Report, DOE/PC/93222-10, March 1996.
[41] L. Gutierrez, A. Boix, J.O. Petunchi, J. Catal. 179 (1998) 179.
[42] R.S. Da Cruz, A.J.S. Mascarenhas, H.M.C. Andrade, Appl. Catal. B 18 (1998) 223.
[43] B.H. Aristizábal, C. Maya, C. Montes de Correa, Appl. Catal. A 335 (2008) 211.
[44] J.Y. Yan, G.-D. Lei, W.M.H. Sachtler, H.H. Kung, J. Catal. 161 (1996) 43.
[45] C.H. Bartholomew, Appl. Catal. A: Gen. 212 (2001) 17.
[46] "Chemical Reaction Engineering", Third Edition, Octave Levenspiel Chapter 21.
[47] S.S. Putluru, J.A. Reddy, Degn, A. Riisager, R. Fehrmann, Catal. Commun. 18 (2012) 41.
[48] P. Budi, R.F. Howe, Catal. Today 38 (1997) 175.
[49] M.J. Rice, A.K. Chakraborty, A.T. Bell, J. Phys. Chem. B 104 (2000) 9987.
[50] H.-Y. Chen, M. El. Malki El, X. Wang, W.M.H. Sachtler, Catalysis by Unique Metal Ion Structures in Solid Matrices NATO Science Series 13 (2001) 75.
[51] M.C. Campa, S. De Rossi, G. Ferraris, V. Indovina, Appl. Catal. B 8 (1996) 315.
[52] M.D. Amiridis, T. Zhang, R. Farrauto, J. Appl. Catal. B 10 (1996) 203.
[53] A. Martinez, S.A. Gomez, G.A. Fuentes, in: C.H. Bartholomew, G.A. Fuentes (Eds.), Catalysis Deactivation, Elsevier, Amsterdam, 1997, pp. 225–230.